Inactivation of two SARS-CoV-2 virus surrogates by electron beam irradiation on large yellow croaker slices and their packaging surfaces

Zonghong Luo [a], Ke Ni [a], Yuancheng Zhou [b], Guanhong Chang [a], Jiangtao Yu [c,**], Chunling Zhang [a], Wenqi Yin [b], Dishi Chen [d], Shuwei Li [b], Shengyao Kuang [b], Peng Zhang [c], Kui Li [c], Junqing Bai [c], Xin Wang [a,*]

[a] College of Food Science and Engineering, Northwest A&F University, Yangling, Shaanxi, 712100, China
[b] Livestock and Poultry Biological Products Key Laboratory of Sichuan Province, Sichuan Animal Science Academy, Chengdu, 610066, China
[c] Yangling Hesheng Irradiation Technologies Co., Ltd., Yangling, Shaanxi, 712100, China
[d] Sichuan Animal Disease Prevention and Control Center, Chengdu, 610041, China

ARTICLE INFO

ABSTRACT

The detection of infectious SARS-CoV-2 in food and food packaging associated with the cold chain has raised concerns about the possible transmission pathway of severe acute respiratory syndrome coronavirus 2 (SARS-CoV-2) in foods transported through cold-chain logistics and the need for novel decontamination strategies. In this study, the effect of electron beam (E-beam) irradiation on the inactivation of two SARS-CoV-2surrogate, viruses porcine epidemic diarrhea virus (PEDV) and porcine transmissible gastroenteritis virus (TGEV), in culture medium and food substrate, and on food substrate were investigated. The causes of virus inactivation were also investigated by transmission electron microscopy (TEM) and Quantitative Real-time PCR (QRT-PCR). Samples packed inside and outside, including virus-inoculated large yellow croaker and virus suspensions, were irradiated with E-beam irradiation (2, 4, 6, 8, 10 kGy) under refrigerated (0 °C)and frozen (−18 °C) conditions. The titers of both viruses in suspension and fish decreased significantly ($P < 0.05$) with increasing doses of E-beam irradiation. The maximum D_{10} value of both viruses in suspension and fish was 1.24 kGy. E-beam irradiation at doses below 10 kGy was found to destroy the spike proteins of both SARS-CoV-2 surrogate viruses by transmission electron microscopy (TEM) and negative staining of thin-sectioned specimens, rendering them uninfectious. E-beam irradiation at doses greater than 10 kGy was also found to degrade viral genomic RNA by qRT-PCR. There were no significant differences in color, pH, TVB-N, TBARS, and sensory properties of irradiated fish samples at doses below 10 kGy. These findings suggested that E-beam irradiation has the potential to be developed as an efficient non-thermal treatment to reduce SARS-CoV-2 contamination in foods transported through cold chain foods to reduce the risk of SARS-CoV-2 infection in humans through the cold chain.

1. Introduction

Since the outbreak of Coronavirus Disease 2019 (COVID-19) in December 2019, it has rapidly escalated into a global pandemic in a very short period. As of November 11, 2020, there have been more than 50 million confirmed cases and 1.2 million deaths (Tsai et al., 2021). COVID-19 not only threatens human health, but also severely stalls global economic development (Chi, Wang, Chen, & Zheng, 2021). COVID-19 is caused by severe acute respiratory SARS-CoV-2, which belongs to a group of Coronaviruses (CoVs) (Valentina Terio & et al.,

2021a, 2021b). CoVs are enveloped viruses with single-stranded-positive-sense RNA and include the genera α, β, γ and δ-CoV (Valentina Terio & et al., 2021a, 2021b), each of which is widely distributed in humans and animals (Tai et al., 2021; Yekta, Vahid-Dastjerdi, Norouzbeigi, & Mortazavian, 2021). SARS-CoV-2 belongs to the β-CoV (Valentina Terio & et al., 2021a, 2021b). Recently, certain human SARS-CoV-2 cases have been associated with imported frozen foods or cold-chain logistics (Spyros, Wei, Joseph, Xiaowei, & L, 2021). Infectious SARS-CoV-2 have been isolated from imported cold-chain foods and their packaging surfaces (Chi et al., 2021; Peipei

---

et al., 2020; Yuan, Kou, Jiang, Li, & Lei, 2020; Yuhua, Shiliang, Caide, & Qingxiu, 2021). In addition, several SARS-CoV-2 cluster infections in cold-chain food sector workers have been reported in many countries (Dyal et al., 2020; Jia et al., 2021). Therefore, the worldwide transmission of SARS-CoV-2 via cold-chain foods should not be ignored (Anelich, Lues, Farber, & Parreira, 2020).

Traditional thermal sterilization technology cannot be applied to cold chain food, while chemical sterilization leads to chemical residues and environmental contamination, and UV irradiation only be used for surface disinfection and prolonged sterilization (Deng et al., 2020). As an effective method to inactivate microorganisms at low temperatures, E-beam irradiation has been proved to be environmentally friendly, effective and convenient (Predmore et al., 2015). E-beam irradiation can be used to sterilize cryogenic or frozen foods to maximize the freshness of cold chain foods. The Food and Agriculture Organization of the United Nations (FAO), the International Atomic Energy Agency (IAEA), the World Health Organization (WHO) and the Scientific Committee on Food of the European Commission (EC) have considered the use of ionizing radiation in food at doses of up to 10 kGy (kGy) (S. E. Kim, S. Y. Park, M.-l. Rui, & S.-D. Ha, 2017; Predmore et al., 2015). As many as 60 countries have approved food irradiation for a variety of foods, including spices, fruits, vegetables, meat and poultry (Sanglay, Li, Uribe, & Lee, 2011). Although the penetration depth of electrons is limited to 2–5 cm (Predmore et al., 2015), they are useful for irradiating large volumes of free-flowing food products, such as cereals or packaged foods such as fish fillets up to 8–10 cm thick with a density of 1 g/cm^3 (Pillai & Shayanfar, 2017).

E-beam irradiation is relatively well established for microbial reduction, but there are few studies on the risk control of SARS-CoV-2in cold chain food, especially in food substrates such as Marine fish and shrimp. In addition, although studies have reported the effects of E-beam irradiation on viral protein and genome, the mechanism of inactivation of enveloped CoVs by E-beam irradiation remains unclear, which is not conducive to the application of E-beam irradiation to control the spread of SARS-CoV-2. Highly infectious viruses, such as the SARS-CoV-2, could compromise the safety of workers or the integrity of the processing environment (Rodriguez, Castell-Perez, Ekpanyaskun, Moreira, & Castillo, 2006), therefore most laboratories use virus surrogates to gain insights into the effects of different treatments on the virus in foods and their production environment (Dellanno, Vega, & Boesenberg, 2009; Perera et al., 2021; Praveen et al., 2013; Sanglay et al., 2011; Singh, Jorgenson, Pringle, Nelson, & Ramamoorthy, 2021a). Surrogates are non-virulent strains of the target pathogen that retain all other characteristics except pathogenicity (Rodriguez et al., 2006). Porcine epidemic diarrhea virus (PEDV) and porcine transmissible gastroenteritis virus (TGEV) belong to the genus α-coronavirus and are single-stranded RNA enveloped viruses with genomes ranging from 25 kb to 32 kb (Meng et al., 2013; Pascual-Iglesias et al., 2019; Singh, Jorgenson, Pringle, Nelson, & Ramamoorthy, 2021b; Yekta et al., 2021; Zhu et al., 2017). Unlike SARS-CoV-2, PEDV and TGEV infect only pigs and can be easily cultured and processed in BSL2 facilities (Singh et al., 2021a). These two viruses are considered good surrogates to SARS-CoV-2 for their biophysiological properties and genomic structure are highly similar compared to SARS-CoV-2 (Liu et al., 2022; Singh et al., 2021b; Zhu et al., 2017).

The aim of this study was to evaluate the inactivation effect of E-beam irradiation on PEDV and TGEV in culture medium and food substrate under refrigerated and frozen conditions, and to determine the inactivation mechanism of surrogate virus by transmission electron microscopy (TEM) observation of ultra-thin sections of cells and negative virus infection and Quantitative Real-time PCR (QRT-PCR). In addition, the quality changes of large yellow croaker treated by E-beam were evaluated.

2. Materials and methods

This study was conducted in compliance with the policies and procedures as approved by Northwest A&F University's institutional biosafety committee.

2.1. Cell culture and virus stock

PEDV strain CV777, TGEV strain SC, Pseudorabies virus strain Fa, Human adenovirus 5 strain SCCD, and cells (Vero cells for PEDV, PK-15 cells for TGEV and Pseudorabies virus, HEK293 cells for Human adenovirus 5) were provided by associate researcher Yuancheng Zhou, Sichuan Animal Science Academy (Chengdu, China). Dulbecco's modified Eagle's medium (DMEM, GIBCO) containing 10% fetal bovine serum (FBS, Gibco, NY, USA), 5% L-glutamine and antibiotics (100 g/mL streptomycin and 100 U/mL penicillin, Beyotime Biotechnology, Shanghai, China) was used for all cell cultures. All cells were cultured at 37 °C with 5% CO$_2$ atmosphere. When the cells achieved 90% confluence in a tissue culture flask, the growth medium was completely removed. A 0.1 multiplicity of infection (MOI) of virus supernatant was added to the flasks and incubated at 37 °C with 5% CO$_2$ atmosphere for 1 h with agitation every 15 min to allow virus adsorption. DMEM containing 2% fetal bovine serum and antibiotics was added to the flasks and they were incubated at 37 °C with 5% CO$_2$ for 3 days. When more than 80% cytopathic effects (CPEs) were observed, the virus-infected flasks were subjected to frozen and thawed 3 times. The viruses' particles were released by cell lysis. After centrifugation at 2500×g for 10 min at 4 °C, the supernatant was subsequently harvested. The titer of the virus stock was 7 or 8 log$_{10}$ TCID$_{50}$/mL and stored at −80 °C for further use. All viruses were cultured and operated in BSL2 facilities, and the virus samples were completely sealed during irradiation. The virus culture supernatant of the 'Pseudorabies virus strain Fa' and 'Human adenovirus 5 strain SCCD′ only used to calculate the virus titration treated and untreated with e-beam irradiation.

2.2. Sample preparation and inoculation

Fresh large yellow croaker was purchased at a seafood market in Yangling City, China and quickly transported on crushed ice to the laboratory at Northwest A&F University (Yangling, Shaanxi, China) and processed within less than 1h. Scales, head, tail, viscera, bones and skin of large yellow croaker were quickly removed in a food laboratory. Large yellow croaker was cleaned with sterile water and then cut into fillets about 100g each along the direction of muscle fibers. 100 g of each fish fillet was cut into litter fillets of about 3 g each. 3 g of large yellow croaker meat was inoculated with a 200 μL of PEDV or TGEV virus suspension and put into a sterile packaging bag. Some parts of inoculated virus samples were stored in crushed ice and other parts were stored at −18 °C for further use. For virus samples in media, each 500 μL of virus suspension was put into a sterile 1.5 mL centrifugal tube and stored at −80 °C for further analysis (Espinosa et al., 2012; S. E. Kim, S. Y. Park, M. L. Rui, & S. D. Ha, 2017; Predmore et al., 2015; Sanglay et al., 2011).

2.3. E-beam irradiation

The samples inoculated with or without PEDV or TGEV and virus culture supernatant were packed in sterile packaging bags as described above and then were placed on the inside and outside surfaces of polystyrene foam incubators (34 × 22 × 18 cm and 30 × 18 × 14.5 cm, 2 cm of wall thickness) containing crushed ice. To ensure a uniform dose, only place samples at a depth of 3–4 cm on ice. During transportation to the irradiation facility, desired temperatures were maintained with dry ice (for samples irradiated frozen) or crushed ice (for samples irradiated refrigeration). The irradiation dose is referred to standard NY/T 1256–2006 of China for electron beam has been slightly

modified. The samples were irradiated by a 10MeV/20 kW high-energy electron linear accelerator (Yangling Hesheng Irradiation Technologies Co., Ltd., Yangling, China) with 0 (unirradiated control), 2.0, 4.0, 6.0, 8.0, and 10.0 kGy. The dose rate of E-beam irradiation is about 4.4 kGy/s, the beam current is 1.6 mA, and the scanning inhomogeneity of equipment is less than 6%. Dose uniformity ratio (DUR) is an important criterion for irradiation experiments. DUR close to 1.0 indicates that the dose in the package is uniform. Dose detection was carried out before the irradiation experiment to ensure uniform dose change of irradiated samples. All treatment groups were replicated at least 3 times. The potassium dichromate (silver) dosimeter was placed on the upper surface of the foam incubator and at sample locations inside the foam incubator to verify the absorbed dose (Table 1). Fig. 1 was a schematic diagram of the E-beam irradiation test.

2.4. Virus recovery

The method of virus recovery was performed as described previously with minor modifications (Espinosa et al., 2012; S. E. Kim & et al., 2017a, 2017b). After irradiation, the large yellow croaker inoculated with or without the virus was soaked in 5 ml of DMEM in a sterile 50-mL centrifugal tube. The samples were thoroughly mixed and shaken at 300 rpm for 1h at room temperature in a rotary shaker (TS-200DC; Tensuc) to elute the virus. After centrifugation at $10,000 \times g$ for 30min at 4 °C, the supernatants were serially filtered using 0.45 and 0.22 μm aseptic filters, and the virus eluent was stored at −80 °C until use.

2.5. Virus titration and D_{10} calculation

Virus titration was calculated by the 50% tissue culture infectious dose (TCID$_{50}$) with the Reed and Muench method as described previously (Dellanno et al., 2009; Schmidt et al., 2012a). Briefly, the 1.5×10^4 cells per well containing 200 μL DMEM supplemented with 10% FBS were seeded in 96-well plates and were incubated at 37 °C with 5% CO$_2$ for 1 day or 2 days to reach 90% confluence before the virus titration. Each eluted solution (viral suspension) was serially diluted 10-fold in DMEM containing 5% FBS. Each dilution was pipetted into quadruplicate wells with Vero cells or PK-15 cells, each well for 200 μL. The plates were incubated at 37 °C with 5% CO$_2$. The cytopathic effects (CPE) were examined for 3 days. TCID$_{50}$ was calculated according to the well number with CPE at each dilution. In this study, the detection limit of virus was 1 TCID50/mL according to the Reed and Muench method. D_{10} calculations were determined by the following formula. The inactivation of viruses often approximates an exponential relationship. Formula (1) was used for the inactivation effect of the virus:

$$D = D10 \times \lg(N_0/N_D) \qquad (1)$$

Where N_0 is the virus titration recovered from unirradiated food matrices and N_D is the virus titration recovered from irradiated food matrices. D is the actual absorbed dose of the irradiated food matrices. D_{10} describes the required absorbed dose to reduce the initial virus titration to 10%. This dose-response curve is based on the assumption of a single-hit-single-target model.

Table 1
Conveyer speed and measured dose on inside and outside surface of polystyrene foam incubators.

Target dose (kGy)	Speed(m/min)	Inside surface (kGy)	Outside surface (kGy)
2.0	10.5	2.31	2.12
4.0	5.3	4.11	4.08
6.0	3.5	6.01	6.10
8.0	2.6	8.30	8.21
10.0	2.1	10.85	10.76

2.6. qRT-PCR analysis

Genomic RNA of E-beam untreated and treated PEDV or TGEV viruses were extracted using miniBEST Viral RNA Exaction Kit Ver.5.0 (TaKaRa). RNA was stored at −80 °C until use. The RNA was reversely transcribed into cDNA using the PrimeScript RT kit (TaKaRa) and stored at −20 °C before use. The primers of qRT-PCR were designed as described previously (Dorlass et al., 2020; Marinowic et al., 2021). PEDV primers included forward primer (5′-GCACTTATTGGCAGGC TTTGT-3′) and reverse primer (5′-CCATTGAGAAAAGAAAGTGTCG TAG-3′). TGEV primers included forward primer (5′-GCTTGATGAATTG AGTGCTGATG-3′) and reverse primer (5′-CCTAACCTCGGCTTGTC TGG-3′). QRT-PCR was performed in a 25 μL reaction mixture using the IQ5 system (Bio-Rad, Hercules, CA, USA) and SYBR premix Ex *Taq*II kit (TaKaRa). QRT-PCR reaction conditions: pre-denaturation at 95 °C for 30s, 40 cycles of denaturation at 95 °C for 5 s, 55 °C annealing for 30s, 72 °C extensions for 30s. Plasmid standards were developed to quantify the copy number of viral RNA. Viral RNA expression was average log$_{10}$ genomic RNA copy number/mL ± standard deviation.

2.7. Transmission electron microscopy (TEM) observation on PEDV and TGEV in cells by ultrathin sectioning

Following TEM observation described previously (Belanger et al., 2011; DiCaprio et al., 2016), Vero cells and PK-15 cells were infected with PEDV and TGEV at 0.1 MOI respectively, when the cytopathic effects (CPEs) was more than 80%, the virus-infected cells treated with serial irradiation doses (0, 4.0, and 10.0 kGy) were collected by centrifugation at 4500g for 10min at 4 °C. The virus-infected cells were fixed using 2.5% glutaraldehyde solution in 0.1 M phosphate-buffered saline (PBS, pH 7.2) at 4 °C for 8h. Glutaraldehyde fixed cells were washed gently three times with PBS for 10 min each time at room temperature. Glutaraldehyde fixed cells were fixed using 1% osmium acid in PBS at 4 °C for 4h. Osmium acid-fixed cells were washed gently three times with PBS. Osmium acid fixed cells were dehydrated using a graded series of ethanol (35%, 50%, 75%, 95% and 100%) for 10 min each time and permeabilized using a graded series of LR-White resin mixed with 100% ethanol (25%, 50%, 75%, 100%, 100%, V/V) for 2, 8, 12h, 24 and 24 h respectively. After percolation, the cells were embedded in pure LR-White resin and cured at 55 °C for 48 h. The 70 nm thin sections were fabricated and mounted on naked copper grids. Ultrathin sections were doubled stained with uranyl acetate and lead citrate.

2.8. Direct TEM observations on PEDV and TGEV by negative staining

When more than 80% cytopathic effects (CPEs) were observed, the virus-infected flasks were subjected to frozen and thawed 3 times. The viruses' particles were completely released by cell lysis. After centrifugation at $4500 \times g$ for 10 min at 4 °C, the supernatant was subsequently harvested. 5 μL of the TGEV and PEDV suspensions treated with 0, 4.0, and 10.0 kGy of e-beam irradiation were added to the surface of the copper net until natural drying. The virus preparation was stained with phosphotungstic acid for 1–3min and observed by TEM.

2.9. Food quality testing

2.9.1. Microbiological analysis
Total viable counts (TVC) of the fresh large yellow croaker samples were measured using plate count agar (PCA, Base Bio-Tech, Hangzhou, China) as described previously (Lan et al., 2020; Lorenzo & Franco, 2012). In this study, the detection limit of total viable counts (TVC) using plate count agar was 1 colony were formed on plate count agar. All counts were performed in duplicate and expressed as log$_{10}$ CFU/g.
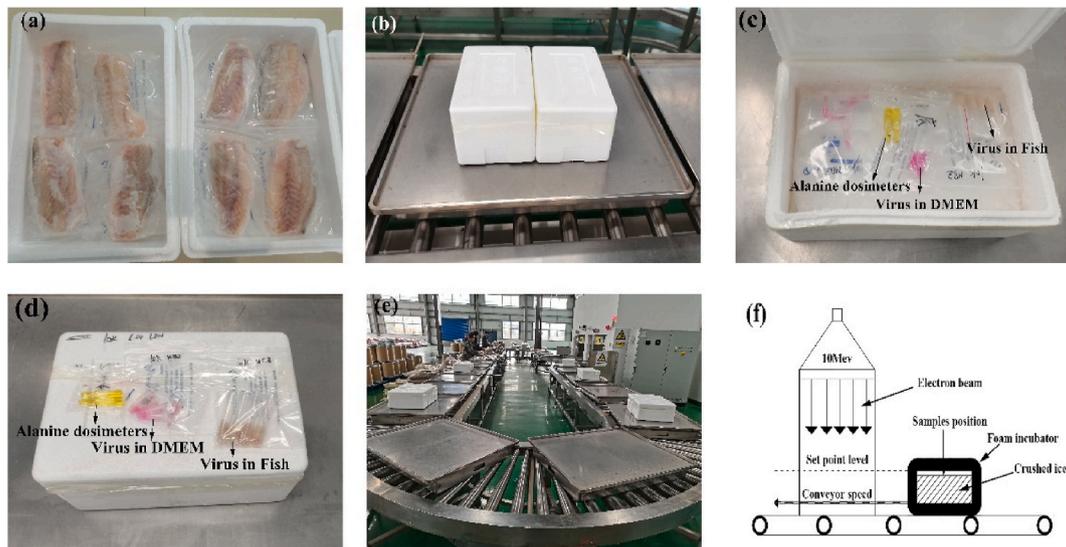
Fig. 1. Schematic diagram of E-beam irradiation.
Fig. 1 (a) is the samples of large yellow croaker in the foam box before irradiation, Fig. 1 (b) is the foam box used for irradiation, Fig. 1 (c) is the virus samples in the foam box before irradiation, Fig. 1 (d) is the virus samples on the outside surface of the foam box before irradiation, and Fig. 1 (e) is the E-beam irradiation workshop. The potassium dichromate (silver) dosimeters were irradiated along with fish and virus samples to measure the actual dose. Fig. 1(f) is schematic of sample packaging and E-beam irradiation process.

2.9.2. Color determination and texture analysis

As described by Zhang et al. (Zhang et al., 2017), color measurements were performed by a colorimeter (X-rite, Shanghai, China) with a 10 mm port size, illuminant D65 and a 10° standard observer. The L* (lightness), a* (red-green), b* (blue-yellow) and ΔE values of fish samples were determined.

Texture analysis was slightly modified as described previously (Sun et al., 2020; Zhang et al., 2017). The texture profile was analyzed by a TA-XT plus texture analyzer (Stable Micro Systems Ltd., UK) with a 50 mm cylindrical probe (P/50). The speeds of pre-test, test and post-test were 3 mm/s, 1 mm/s and 3 mm/s, respectively. In addition, the trigger force and strain distance are 5 g and 5 mm, respectively.

2.9.3. pH value

The pH value was determined by the method of Zhang et al. (Zhang et al., 2017). Briefly, 5 g of each sample treated with serial irradiation doses (0, 2.0, 4.0, 6.0, 8.0, and 10.0 kGy) was aseptically placed into a sterile homogenizing bag containing 50 ml sterile deionized water and homogenized for 5 min using a DH-11L Homogenizer. The pH of each sample was measured using a pH meter (PHS–3C, Leici Company, Shanghai, China) in triplicate at room temperature.

2.9.4. Total volatile basic nitrogen (TVB-N) determination

The determination of TVB-N values was obtained by Conway's micro-diffusion method. Briefly, 20 g of each sample treated with serial irradiation doses (0, 2.0, 4.0, 6.0, 8.0, and 10.0 kGy) was aseptically placed into a sterile homogenizing bag containing 100 ml sterile deionized water and homogenized for 5 min using a DH-11L Homogenizer. The homogenized samples were centrifuged and filtered to collect the supernatants. The supernatants were analyzed using Conway's micro-diffusion method. TVB-N values were expressed as mg N/100 g.

2.9.5. Thiobarbituric acid-reactive substances (TBARS) analysis

TBARS was determined by spectrophotometry based on the method of Sun et al. (Sun et al., 2020). The TBARS values were expressed as mg malonaldehyde (MDA)/kg.

2.9.6. Sensory evaluation

The sensory evaluation of large yellow croaker samples was slightly

modified as described previously (Palotás, Palotás, Jónás, Lehel, & Friedrich, 2020). The evaluation team was composed of 10 professional evaluators (5 male and 5 female). Before the test, the evaluators were not allowed to eat irritating food within 5 h. For sensory evaluation of general appearance, color, odor, and texture, raw fish samples of treated and untreated with E-beam irradiation were removed from cold storage (0 °C and −18 °C) and equilibrated at room temperature (25 °C) for 1 h before evaluation. The color, odor, texture and general acceptability of the samples were scored and evaluated comprehensively. The sensory evaluation was based on a 5-point hedonic scale: 1, Failed; 2, Limited consumption qualities; 3, Medium; 4, Good; 5, Very good. Due to the unknown results of the microbiological analysis, it was only performed on day 0 for food safety reasons.

2.9.7. Electronic nose analysis

Electronic nose analysis was proceeded based on the reported methods with slight modification (Grassi, Benedetti, Opizzio, Nardo, & Buratti, 2019; Vajdi, Varidi, Varidi, & Mohebbi, 2019). 3g of each fish sample was placed in a brown bottle, sealed by sealing film, and placed at room temperature for 30 min to equilibrate the headspace volatile compounds. PEN3 electronic nose (AIRSENSE, Germany) was used to measure the response value of volatile compounds of the samples in triplicate. The measurement parameters were set as follows: cleaning process for 300s, a pre-injection process for 5s, detection process for the 60s, the injection flow rate at 300 mL/min, and carrier gas flow rate at 300 mL/min. After the response values of the electronic nose were obtained, principal component analysis (PCA) was performed using the Win Muster software for the volatile odor of the samples.

2.10. Statistical analysis

Microsoft Excel 2019, Origin 8.5 and SPSS Statistics 18.0 (IBM Corp., Armonk, NY) were used to analyze experimental data. Data were expressed as mean ± SD. Bacterial numbers in CFU/g were converted to log_{10} for statistical analysis. The differences between the different dose groups were analyzed using the Duncan program of variance (ANOVA). $P < 0.05$ was considered a statistically significant difference.

3. Results

3.1. Effect of E-beam irradiation on virus activity

As shown in (Fig. 2A) and (Fig. 2B), the titer of PEDV and TGEV on the outside surface of the foam at 2.12 kGy of E-beam application was reduced by 2.85 ± 0.14 and 2.73 ± 0.04 log10 in DMEM, and by 2.58 ± 0.18 and 2.48 ± 0.39 log10 in fish, respectively. The titer of PEDV and TGEV on the inside surface of the foam at 2.31 kGy of E-beam was reduced by 1.88 ± 0.18 and 2.60 ± 0.21 log10 in DMEM and by 3.00 ± 0.35 and 1.88 ± 0.18 log in fish, respectively. The titers of two surrogate viruses decreased significantly ($P < 0.05$) in the irradiated groups compared with the non-irradiated control groups. Two viruses were not detected by Reed and Muench method at doses of 4.08 kGy and higher (Not shown in Fig. 2). As shown in Table 2, both PEDV and TGEV showed high irradiation sensitivity (maximum $D_{10} = 1.24$ kGy), and there were significant differences between the two viruses in different media (DMEM and Fish) in the inside package ($P < 0.05$).

3.2. Quantitative reverse transcription PCR

Fig. 3 illustrates the effect of E-beam irradiation on viral RNA genomes. For PEDV and TGEV on the inside and outside surface of the foam (Fig. 3A), the changes in genomic RNA of the two viruses were not significant within the dose of 10 kGy ($P > 0.05$). The level of RNA of the two SARS-CoV-2 surrogate viruses reduced significantly ($P < 0.05$) at more than 10 kGy (Fig. 3B). The level of RNA decreased by more than 2 $\log_{10}$ copies/μL when the E-beam irradiation dose was 30 kGy, especially the PEDV RNA level decreased significantly ($P < 0.05$).

3.3. Effect of E-beam on virus structure

The effect of different irradiated doses on the structure of PEDV in Vero cells and TGEV in PK-15 cells were observed by TEM (Tecnai G2 F20 U-Twin, FEI, USA or EM-1230, JEOL, Japan) (Fig. 4) using ultrathin sectioning. The unirradiated viral particles of PEDV and TGEV were spherical or oval in shape, the viral diameters were in the range of 45–100 nm, some viral particles are electron opaque halo or electron-dense cores, however the spike proteins were not obvious (Fig. 4a and d). As the irradiation dose increased, the irradiated viral particles of PEDV and TGEV were also spherical or oval in shape, but the virus particles were more seriously damaged (Fig. 4b and e), and the viral average diameters were in 57, 77 and 60 nm at 0, 4.0 and 10.0 kGy, respectively (Fig. 2C). The spike proteins of the two viruses became more obviously with the increase of irradiation dose (Fig. 4c and f).

Table 2
D_{10} values of PEDV and TGEV in DMEM and virus-inoculated Large yellow croaker by E-beam irradiation.

Treatment	D_{10} value(kGy)	
	PEDV	TGEV
Inside surface (DMEM)	1.24 ± 0.12^a	0.89 ± 0.07^b
Inside surface (Fish)	0.78 ± 0.09^b	1.24 ± 0.11^a
Outside surface (DMEM)	0.74 ± 0.04^b	0.78 ± 0.01^b
Outside surface (Fish)	0.82 ± 0.07^b	0.87 ± 0.13^b

Values are mean $\pm$ SD. Different lowercase letters in different groups indicate a significant difference ($P < 0.05$, n = 3).

Table 3
The sensitivity of irradiated viruses with different diameters and type of virus.

Type of virus		Diameter (nm)	D_{10} value of irradiation
Enveloped virus	Pseudorabies virus	150 to 200	5.7 ± 0.14^a
	PEDV	45 to 100	1.24 ± 0.12^b
	TGEV	45 to 82	1.24 ± 0.11^b
Non-enveloped virus	Human Adenovirus-5	65 to 80	4.0 ± 0.27^c

Values are mean $\pm$ SD. Different lowercase letters in different groups indicate a significant difference ($P < 0.05$, n = 3).

TEM with negative staining showed that the prominent spikes on coronavirus particles were very clear in the unirradiated PEDV and TGEV supernatant samples, showing a typical coronavirus structure (Fig. 5). The diameter of the virus particle is about 100 nm (Fig. 5a and d). However, with the increase of radiation dose, the damage of spikes on coronavirus particles become more and more serious, and the typical coronavirus structure become less and less obvious (Fig. 5c and f).

3.4. Quality evaluation of large yellow croaker after irradiation

3.4.1. Microbial analysis of irradiated large yellow croaker

As shown in Table 4, the total number of microorganisms in refrigerated and frozen large yellow croaker without irradiation is 4.77 $\log_{10}$ CFU/g and 4.54 $\log_{10}$ CFU/g, respectively. No microorganisms were detected in fish of different irradiation dose groups after E-beam irradiation.

3.4.2. Color, texture, sensory evaluation and electronic nose analysis of irradiated large yellow croaker

Fig. 6 showed that there is no significant difference in a* value, b*
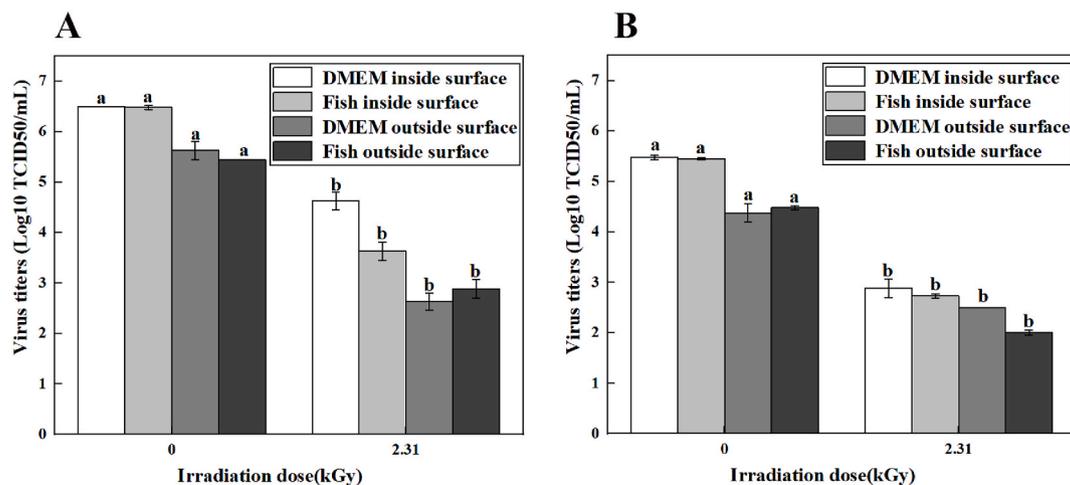
Fig. 2. Virus titers of PEDV(A) and TGEV(B) in large yellow croaker and DMEM samples by E-beam irradiation. Different lowercase letters in different groups indicate a significant difference ($P < 0.05$, n = 3).
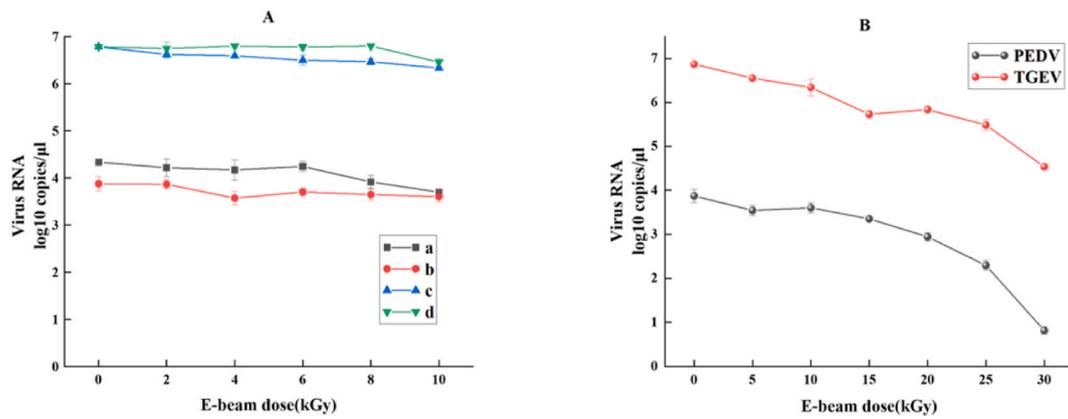
Fig. 3. Copy number of viral RNA detected by quantitative Real-time PCR in DMEM and fish.
(A) Viral RNA copy numbers at different irradiation doses (2, 4, 6, 8, 10 kGy, 0 kGy for control group). The a indicates PEDV viral RNA copy numbers inside the package; b indicates PEDV viral RNA copy numbers outside the package; c indicates TGEV viral RNA copy numbers inside the package; d indicates TGEV viral RNA copy numbers outside the package. (B) RNA copy numbers of two viruses at different irradiation doses (5, 10, 15, 20, 25, 30 kGy, 0 kGy is the control group). All tests were repeated three times.
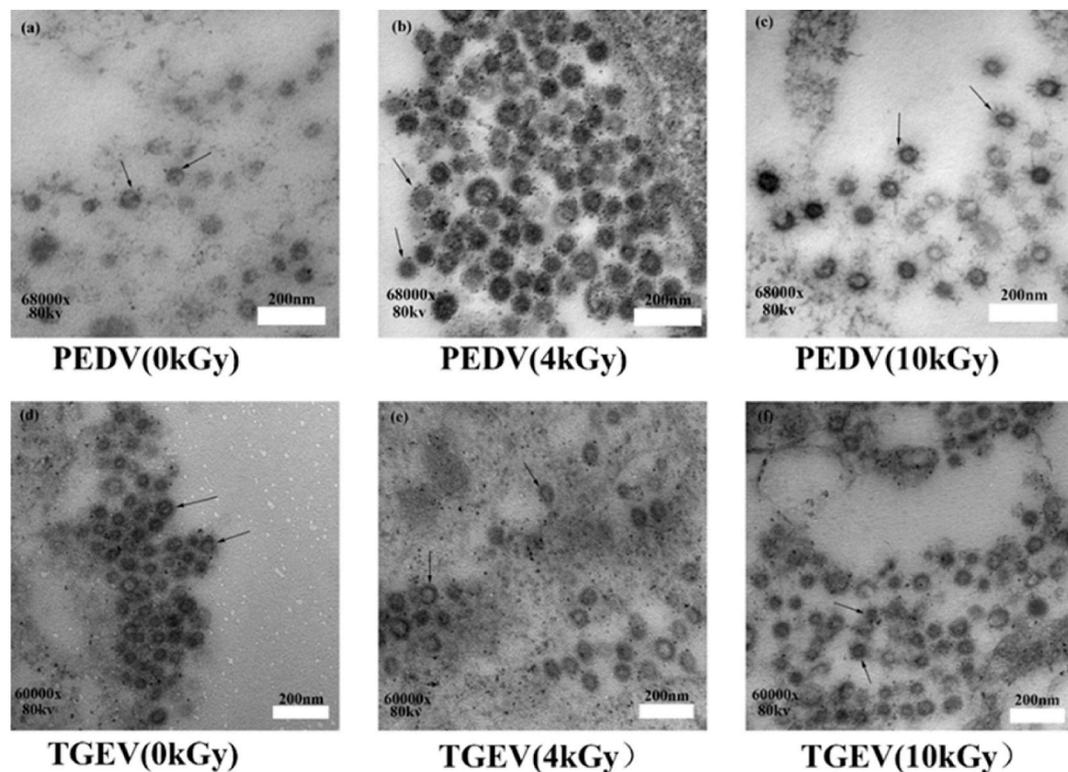
Fig. 4. Transmission electron microscope observation on PEDV in Vero cells and TGEV in PK-15 cells by ultrathin sectioning
a、b、c were PEDV treated with 0, 4.0, and 10.0 kGy of E-beam irradiation, respectively; d, e and f were TGEV treated with 0, 4.0, and 10.0 kGy of E-beam irradiation, respectively. The arrow direction is the fibrin out of the envelope of the virus.

value and ΔE values between refrigerated and frozen large yellow croakers at different irradiation doses. L* value of refrigerated large yellow croaker at different doses shows no difference, while it fluctuates slightly under frozen conditions.

As shown in Table 5, the texture of both refrigerated and frozen large yellow croakers had significant changes with the change of irradiation dose, but it was not obvious when the irradiation dose was less than 6 kGy, and the texture changes were mainly concentrated in the high-dose groups of 8.30 kGy and 10.85 kGy.

Fig. 7 showed the sensory characteristics and overall acceptability of large yellow croakers under different irradiation doses. The sensory

evaluation results showed that the color and texture of large yellow croakers under different irradiation doses have no significant difference. The overall acceptability of sensory evaluation of irradiated fish was not significantly different below 8.30 kGy.

Fig. 8 showed the 2D diagram of the electronic nose principal component analysis, in which PC1 and PC2 contributed 73.2% of the data variance. Fig. 8 also showed that the electronic nose can distinguish between refrigerated and frozen large yellow croakers, but the linear distances on PC1 and PC2 of large yellow croakers are close between different irradiation doses.
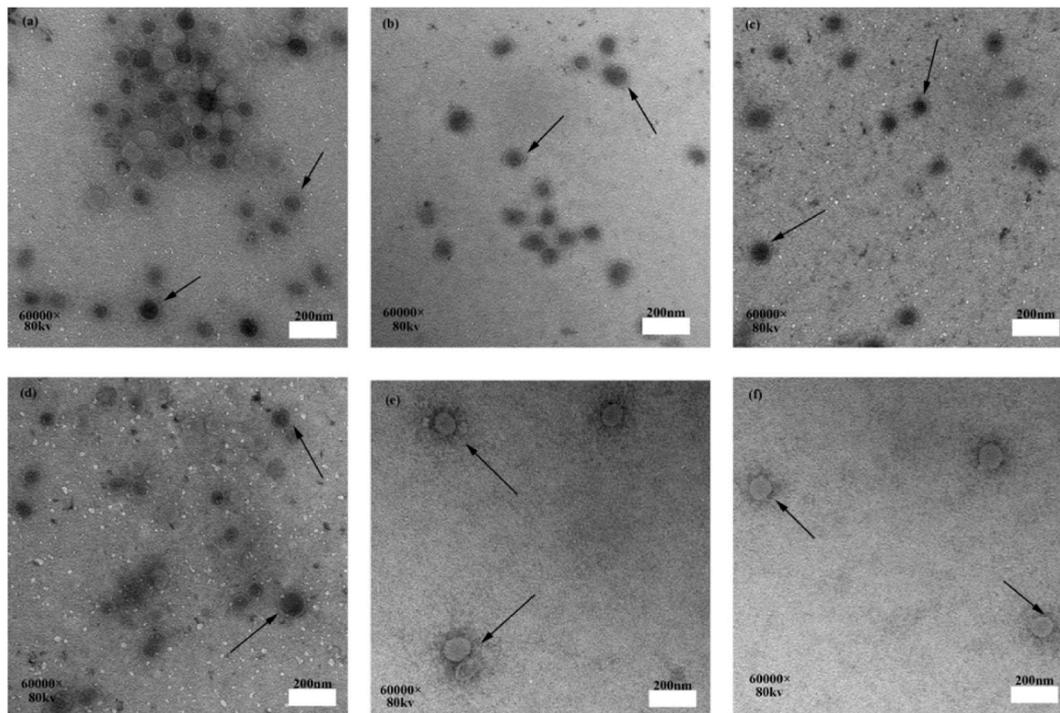
Fig. 5. Transmission electron microscopy observation on PEDV and TGEV by negative staining

a、b、c were PEDV treated with 0, 4.0, and 10.0 kGy of E-beam irradiation, respectively; d, e and f were TGEV treated with 0, 4.0, and 10.0 kGy of E-beam irradiation, respectively. The arrow direction is the fibrin out of the envelope of the virus.

Table 4
Effects of microbe number of large yellow croaker with irradiation.

E-beam irradiation dose(kGy)	Microorganisms/($\log_{10}$ CFU/g± SD)	
	Refrigeration	Freezing
0	4.77 ± 0.10 [a]	4.54 ± 0.09 [a]
2.31	ND	ND
4.11	ND	ND
6.01	ND	ND
8.30	ND	ND
10.85	ND	ND

Different lowercase letters in different groups indicate a significant difference ($P < 0.05$, n = 3). ND Indicates not detected.

3.4.3. Effects of E-beam on pH, TBARS and TVB-N of irradiated large yellow croaker

As shown in Fig. 9, there was no significant difference in both pH (Fig. 9C) and TVB-N (Fig. 9B) of large yellow croaker with and without irradiation in refrigerated or frozen conditions ($P > 0.05$), and the trends did not change with and without irradiation. The TBARS (Fig. 9A) values of large yellow croaker in refrigerated and frozen conditions have a significant influence on E-beam irradiation ($P < 0.05$), and the change trends were similar in refrigerated and frozen conditions.

4. Discussion

The presence of SARS-CoV-2 in cold-chain foods has been demonstrated, suggesting that the virus may occur in communities and may be
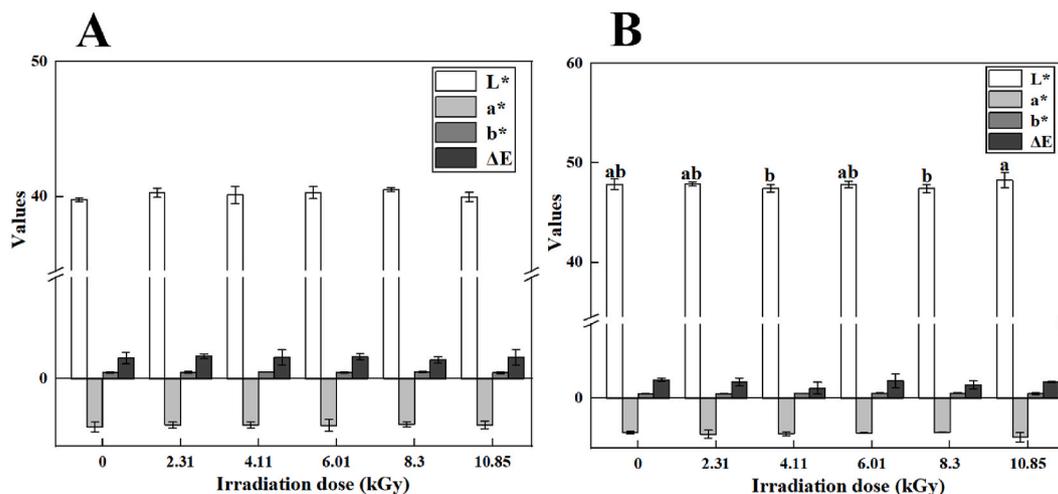
Fig. 6. Color values (L*a*b*ΔE) of refrigeration (A) and freezing (B) large yellow croaker by E-beam irradiation. Different lowercase letters in different groups indicate a significant difference ($P < 0.05$, n = 3).

Table 5
TPA of large yellow croaker by E-beam irradiation. Changes in texture were measured by hardness, adhesiveness, springiness, cohesiveness, gumminess, chewiness and resilience.

Treatment	E-beam irradiation dose (kGy)	Hardness(g)	Adhesiveness (g)	Springiness (%)	Cohesiveness (%)	Gumminess(g)	Chewiness(g)	Resilience (%)
Refrigeration	0	151.30 ± 6.98 [b]	−9.79 ± 1.41 [c]	0.85 ± 0.01 [ab]	0.56 ± 0.03[ab]	80.32 ± 2.41[a]	70.37 ± 3.82[a]	0.20 ± 0.00[a]
	2.31	162.56 ± 4.69 [a]	−6.12 ± 2.7 [ab]	0.81 ± 0.01 [b]	0.56 ± 0.02[ab]	80.31 ± 1.25[a]	69.89 ± 6.42[a]	0.23 ± 0.01[a]
	4.11	165.98 ± 8.39[a]	−6.27 ± 1.97[ab]	0.86 ± 0.04[ab]	0.55 ± 0.05[ab]	80.28 ± 5.65[a]	70.38 ± 2.94[a]	0.19 ± 0.01[a]
	6.01	170.77 ± 6.67[a]	−7.17 ± 0.84[ab]	0.88 ± 0.02[a]	0.57 ± 0.03[ab]	80.29 ± 8.36[a]	70.37 ± 2.65[a]	0.22 ± 0.06[a]
	8.30	140.46 ± 2.86[c]	−8.48 ± 1.08[bc]	0.84 ± 0.05[ab]	0.57 ± 0.01[ab]	80.44 ± 1.96[a]	70.22 ± 2.96[a]	0.22 ± 0.02[a]
	10.85	117.20 ± 2.95[de]	−4.44 ± 0.30[a]	0.81 ± 0.04b	0.53 ± 0.03b	80.19 ± 0.27a	70.58 ± 3.80[a]	0.20 ± 0.03a
Freezing	0	82.37 ± 2.50[g]	−4.87 ± 1.17[a]	0.83 ± 0.01[ab]	0.58 ± 0.01[ab]	47.59 ± 0.79[e]	37.29 ± 4.57[c]	0.20 ± 0.02[a]
	2.31	81.81 ± 0.99[g]	−4.91 ± 2.45[a]	0.85 ± 0.04[ab]	0.58 ± 0.01[a]	47.12 ± 0.99[e]	42.58 ± 1.80[c]	0.21 ± 0.01[a]
	4.11	98.22 ± 1.75[f]	−5.20 ± 0.47[a]	0.84 ± 0.03[ab]	0.59 ± 0.02[a]	59.35 ± 2.72[d]	55.24 ± 10.40[b]	0.24 ± 0.01[a]
	6.01	123.67 ± 12.24[d]	−5.12 ± 0.27[a]	0.87 ± 0.00[a]	0.55 ± 0.03[ab]	67.74 ± 5.58[bc]	56.86 ± 7.63[b]	0.21 ± 0.02[a]
	8.30	164.04 ± 6.27[a]	−4.84 ± 0.24[a]	0.86 ± 0.03[ab]	0.58 ± 0.01[ab]	71.08 ± 2.86[b]	54.23 ± 2.46[b]	0.20 ± 0.00[a]
	10.85	11.84 ± 6.16[e]	−8.12 ± 1.07[bc]	0.83 ± 0.04[ab]	0.55 ± 0.01[ab]	61.34 ± 4.27c[d]	55.23 ± 4.10[b]	0.22 ± 0.02[a]

Values are mean ± SD. Different lowercase letters in different groups indicate a significant difference ($P < 0.05$, n = 3).
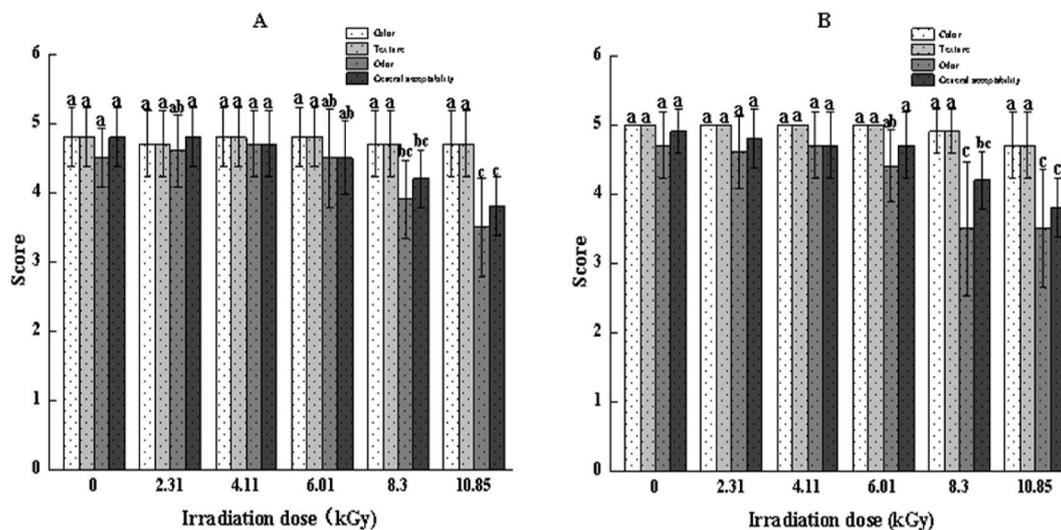
Fig. 7. Sensory evaluation of irradiated refrigeration (A) and freezing (B) large yellow croaker. Different lowercase letters in different groups indicate a significant difference ($P < 0.05$, n = 3).

transmitted in humans through the outer and inner packaging of imported cold-chain foods (Adrián, Yeşim, & R, 2021; Anelich et al., 2020; Chin et al., 2020; Peipei et al., 2020; Yekta et al., 2021). E-beam irradiation is an effective non-thermal sterilization technique to enhance the safety and quality of food (Deng et al., 2020). It has high applicability to disinfect the virus in cold-chain food and food packaging surfaces (Aguirre, Rodriguez, & Garcia de Fernando, 2011; Arvanitoyannis, Stratakos, & Mente, 2009; Feng, Liu, Cui, & Wang, 2020; R. K. Gautam & Venugopal, 2021; M & M, 2006; Mousavi Khaneghah, Hashemi Moosavi, Oliveira, Vanin, & Sant'Ana, 2020; Su, Duan, & Morrissey, 2004). In addition, due to the high pathogenicity of SARS-CoV-2in humans, most laboratories assess the inactivation of the virus by using virus surrogates in the food processing chain (Dellanno et al., 2009; Meyer et al., 2020; Perera et al., 2021; Predmore et al., 2015; Sanglay et al., 2011; Singh et al., 2021a; Valentina Terio & et al., 2021a, 2021b). Therefore, in this study, the inactivation effect of two surrogate viruses in DMEM and food matrices and the causes of virus inactivation were assessed by low-temperature E-beam irradiation to provide ideas for controlling SARS-CoV-2 contamination in cold chain products.

According to Liu et al.' study, an irradiation dose of 10 kGy reduced the PEDV virus titer by 1.68–1.76 log10 TCID50/100 μL in a cold-chain environment (−20 °C) (Liu et al., 2022). In this study, the D_{10} values of PEDV and TGEV in DMEM and virus-inoculated Large yellow croaker are all less than 2 kGy (Table 2). Moreover, electron beam irradiation at >4 kGy completely inactivated PEDV and TGEV in the specimens (0 °C). This is mainly because electron beam irradiation is essentially the irradiation of water, leading to the formation of free radicals (Raj Kamal Gautam & Vazhiyil Venugopal, 2021), and the presence of liquid water in DMEM and fish meat contributes to the diffusion of free radicals in the specimens, resulting in significant radiolytic changes (Raj Kamal Gautam & Vazhiyil Venugopal, 2021). Previous studies have reported differences in the resistance of enveloped and non-enveloped viruses to the environment (Moore, 2012; Schmidt et al., 2012b). As shown in Table 3, the two enveloped viruses irradiated in this study (PEDV and TGEV) had significantly lower D_{10} values than non-enveloped viruses, and both enveloped and non-enveloped viruses have capsid proteins (Pascual-Iglesias et al., 2019; Pomeranz, Reynolds, & Hengartner, 2005), suggesting that the capsid protein may not be strongly correlated with CoVs inactivation. However, the D_{10} values of pseudorabies virus were significantly higher than those of non-enveloped viruses. In terms of viral structure, CoVs (PEDV and TGEV) have a specific spike structure on the envelope surface compared to pseudorabies virus (Pascual-Iglesias
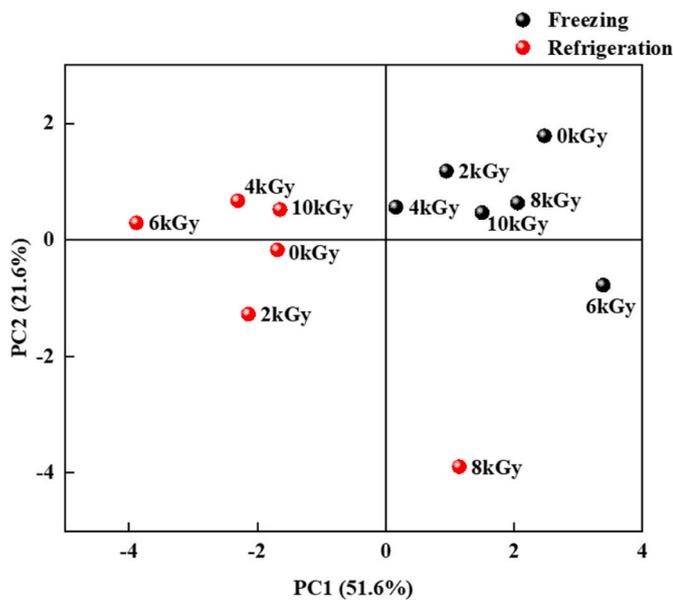
Fig. 8. 2-dimensional principal component analysis of irradiated large yellow croaker.

et al., 2019; Pomeranz et al., 2005), which raised our focus on the spike structure of CoVs.

PEDV and TGEV are structurally similar to SARS-CoV-2 according to previous reports (Liu et al., 2022; Singh et al., 2021b; Zhu et al., 2017).

Their genomes encode three structural proteins: spike (S) glycoprotein, envelope (E) protein, and membrane (M) protein (Tai et al., 2021). Circular, elliptical or polymorphic virus particles and their internal structure, consisting of an electron-dense core and an electron-opaque corona (corona-like), were observed by TEM. The corona-like shape is S proteins with cilia for 16–24 nm (Cui, Theuns, Xie, Van den Broeck, & Nauwynck, 2020; Yao et al., 2020). S protein is a type-I glycoprotein, a key protein for coronavirus infection of host cells, and destruction of this protein structure prevent virus transmission (Cui et al., 2020; R et al., 2021; Yao et al., 2020). TEM and negative staining with thin-section specimens showed significant cosmetic damage to the S protein on PEDV and TGEV viral outside membranes at low irradiation doses in this study, while no significant damage was observed to the viral envelope. Moreover, no significant changes in nucleic acid were detected at low irradiation dose conditions (≤10 kGy), and only at high irradiation dose conditions (>10 kGy) did the viral nucleic acid change. However, the surrogate viruses were already inactivated under the irradiation of 4 kGy E-beam, suggesting that RNA degradation may not be responsible for the inactivation of both CoVs by the E-beam. Schmidt et al. reported that free radical interactions generated by electron beam irradiation may damage viral protein (Schmidt et al., 2012b). Therefore, the damage to the S protein of PEDV and TGEV may be responsible for their loss of infectivity. The inactivation mechanism of SARS-CoV-2 by E-beam irradiation may also be damage of the S protein, which may contribute to the investigate of SARS-CoV-2inactivation by E-beam irradiation.

The dose of E-beam irradiation used to control the risk of SARS-CoV-2 infection and microbial contamination must be within the limits that do not adversely affect food quality. According to previous studies, the effect of irradiation is essentially the radiolysis of water resulting in the
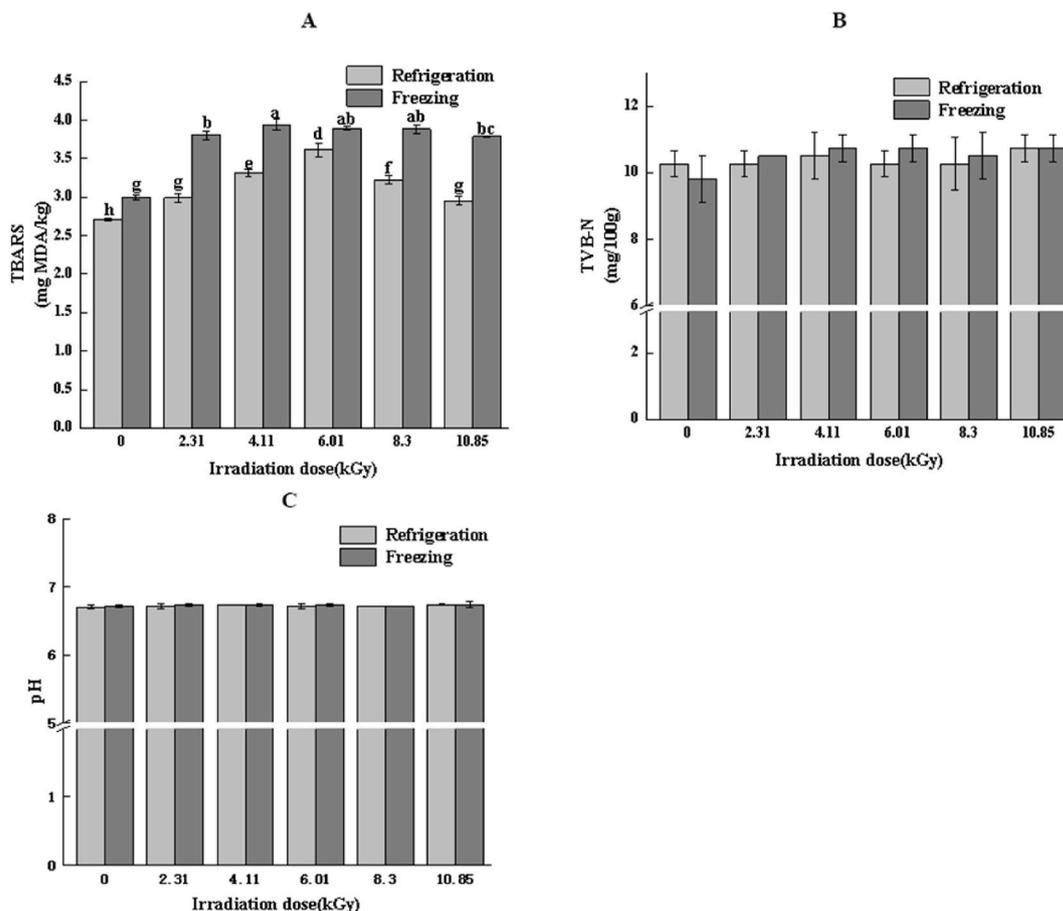
Fig. 9. TBARS (A), TVB-N (B) and pH (C) of large yellow croaker by E-beam irradiated. Different lowercase letters in different groups indicate a significant difference (*P* < 0.05, n = 3).

formation of free radicals and ozone (Raj Kamal Gautam & Vazhiyil Venugopal, 2021; Pillai & Shayanfar, 2017). The free radicals and ozone could induce lipid and protein oxidation (Zhang et al., 2017), resulting in color and odor changes in fish (Badr, 2012; Yagiz et al., 2010). In addition, Zhang et al. reported the effects of 3 kGy irradiation on the microorganism, color, pH, TBARS and sensory quality of carp slices stored at 4 °C (Zhang et al., 2017). Sensory characteristics and general acceptability are associated with spoilage bacteria growth and lipid oxidation (Zhang et al., 2017), while electronic nose can assess fish freshness (Grassi et al., 2019). Thus, the qualities of large yellow croakers were evaluated at different E-beam irradiation doses. To facilitate the test, the entire back muscle of the large yellow croaker was selected to characterize the effect of e-beam irradiation on the quality of the large yellow croaker. Because the large yellow croaker is usually sold as a whole fish, this setup may have some limitations. According to the International Committee on Microbiological Specifications for Food of the International Federation of Societies for Microbiology (ICMSF), the acceptable limit for microorganisms in fish is 5.7 log CFU/g. In this study, no microorganisms were detected in the samples at different irradiation doses after E-beam irradiation, thus fully satisfying the ICMSF microbial limit. There were no significant differences ($P < 0.05$) in color, texture and sensory qualities of the samples treated with different irradiation doses compared to untreated samples in this study, which is consistent with the results of previous studies (Sun et al., 2020; Zhang et al., 2017). In addition, there were no significant differences in pH and TVB-N of samples treated with different radiation doses, and TBARS remained within an acceptable limits (Sun et al., 2020). These results suggested that low dose E-beam irradiation did not significant affect on the qualities of large yellow croakers but did significantly inactivate microorganisms in large yellow croakers ($P < 0.05$).

5. Conclusion

Through our study, we concluded that: (1) Damage to extra-membrane fibronectin (S protein) maybe the mechanism of the inactivation of the replacement virus by E-beam irradiation. (2) Degradation of viral genomic RNA may not be the cause of the E-beam inactivation of the enveloped virus, because the viral genomic RNA was not significantly degraded at low irradiation dose ($\leq$10 kGy) but only changed at high irradiation dose ($>$10 kGy), while the virus was inactivated at 4 kGy irradiation. (3) Both SARS-CoV-2 surrogates were completely inactivated by E-beam irradiation at 4 kGy, while the qualities of large yellow croaker did not change significantly within 10 kGy of E-beam irradiation. (4) E-beam technology can be used to inactivate SARS-CoV-2 on the inside and outside surfaces of cold chain food packaging, reducing the SARS-CoV-2 infection risk for humans through the cold chain. The preliminary recommended safe E-beam irradiation dose is 4–6 kGy.

CRediT authorship contribution statement

Zonghong Luo: Conceptualization, Methodology, Validation, Writing – original draft, Visualization, Investigation. **Ke Ni:** Investigation, Validation, Supervision, Writing – review & editing. **Yuancheng Zhou:** Investigation, Validation, Supervision, Writing – review & editing. **Guanhong Chang:** Investigation, Validation, Supervision, Writing – review & editing. **Jiangtao Yu:** Investigation, Validation, Supervision, Writing – review & editing. **Chunling Zhang:** Investigation, Validation, Supervision, Writing – review & editing. **Wenqi Yin:** Validation, Supervision, Writing – review & editing. **Dishi Chen:** Validation, Supervision, Writing – review & editing. **Shuwei Li:** Validation, Supervision, Writing – review & editing. **Shengyao Kuang:** Validation, Supervision, Writing – review & editing. **Peng Zhang:** Supervision, Writing – review & editing. **Kui Li:** Supervision, Writing – review & editing. **Junqing Bai:** Validation, Supervision, Writing – review & editing. **Xin Wang:** Conceptualization, Methodology, Supervision, Visualization,

Investigation, Writing – review & editing, Project administration, Funding acquisition.

Declaration of competing interest

The authors declare that there are no conflicts of interest.

Data availability

Data will be made available on request.

Acknowledgements

References

Adrián, P., et al. (2021). A critical review of disinfection processes to control SARS-CoV-2 transmission in the food industry. *Foods, 10*(2), 283–299. https://doi.org/10.3390/foods10020283

Aguirre, J. S., et al. (2011). Effects of electron beam irradiation on the variability in survivor number and duration of lag phase of four food-borne organisms. *International Journal of Food Microbiology, 149*(3), 236–246.

Anelich, L., et al. (2020). SARS-CoV-2 and risk to food safety. *Frontiers in Nutrition, 7*, 580551–580559.

Arvanitoyannis, I. S., et al. (2009). Impact of irradiation on fish and seafood shelf life: A comprehensive review of applications and irradiation detection. *Critical Reviews in Food Science and Nutrition, 49*(1), 68–112.

Badr, H. M. (2012). Control of the potential health hazards of smoked fish by gamma irradiation. *International Journal of Food Microbiology, 154*(3), 177–186.

Belanger, J. M., et al. (2011). Effects of UVA irradiation, aryl azides, and reactive oxygen species on the orthogonal inactivation of the human immunodeficiency virus (HIV-1). *Virology, 417*(1), 221–228.

Chi, Y., et al. (2021). The long-term presence of SARS-CoV-2 on cold-chain food packaging surfaces indicates a new COVID-19 winter outbreak: A mini review. *Frontiers in Public Health, 9*, 650492–650502.

Chin, A. W. H., et al. (2020). Stability of SARS-CoV-2 in different environmental conditions. *Lancet Microbe, 1*(4), 30093–30098.

Cui, T., et al. (2020). Role of porcine aminopeptidase N and sialic acids in porcine coronavirus infections in primary porcine enterocytes. *Viruses, 12*(4), 402–420.

Dellanno, C., et al. (2009). The antiviral action of common household disinfectants and antiseptics against murine hepatitis virus, a potential surrogate for SARS coronavirus. *American Journal of Infection Control, 37*(8), 649–652.

Deng, L. Z., et al. (2020). Emerging chemical and physical disinfection technologies of fruits and vegetables: A comprehensive review. *Critical Reviews in Food Science and Nutrition, 60*(15), 2481–2508.

DiCaprio, E., et al. (2016). Inactivation of human norovirus and Tulane virus in simple media and fresh whole strawberries by ionizing radiation. *International Journal of Food Microbiology, 232*, 43–51.

Dorlass, E. G., et al. (2020). Lower cost alternatives for molecular diagnosis of COVID-19: Conventional RT-PCR and SYBR green-based RT-qPCR. *Brazilian Journal of Microbiology, 51*(3), 1117–1123.

Dyal, J. W., et al. (2020). COVID-19 among workers in meat and poultry processing facilities. *US Department of Health and Human Services/Centers for Disease Control and Prevention, 69*(18), 557–561.

Espinosa, A. C., et al. (2012). Quantifying the reduction in potential health risks by determining the sensitivity of poliovirus type 1 chat strain and rotavirus SA-11 to electron beam irradiation of iceberg lettuce and spinach. *Applied and Environmental Microbiology, 78*(4), 988–993.

Feng, G., et al. (2020). Electron beam irradiation on novel coronavirus (COVID-19): A monte–Carlo simulation. *Chinese Physics B, 29*(4), 048703-048707.

Gautam, R. K., & Venugopal, V. (2021). Electron beam irradiation to control biohazards in seafood. *Food Control, 130*, 108320–108330.

Grassi, et al. (2019). Meat and fish freshness assessment by a portable and simplified electronic nose system (mastersense). *Sensors, 19*(14), 3225–3240.

Jia, J., et al. (2021). [Investigation of contamination of SARS-CoV-2 in imported frozen seafood from a foreign cargo ship and risk factors for infection in stevedores in Qingdao]. *Zhonghua Liuxingbingxue Zazhi, 42*(8), 1360–1364.

Kim, S. E., et al. (2017a). Effects of electron beam irradiation on murine norovirus-1 in abalone (Haliotis discus hannai) meat and viscera. *Lebensmittel-Wissenschaft & Technologie, 86*, 611–618.

Kim, S. E., et al. (2017b). Effects of electron beam irradiation on murine norovirus-1 in abalone (Haliotis discus hannai) meat and viscera. *LWT - Food Science and Technology, 86*, 611–618.

Lan, W. Q., et al. (2020). Effects of ε·olylysine and rosemary extract on the quality of large yellow croaker (Pseudosciaena crocea) stored on ice at 4 ± 1°C. *Journal of Food Biochemistry, 44*(10), 13418–13429. https://doi.org/10.1111/jfbc.13418

Liu, Y., et al. (2022). Inactivation of porcine epidemic diarrhea virus with electron beam irradiation under cold chain conditions. *Environmental Technology & Innovation, 27*, 102715–102760. https://doi.org/10.1111/jfbc.13418

Lorenzo, J. M., & Franco, D. (2012). Fat effect on physico-chemical, microbial and textural changes through the manufactured of dry-cured foal sausage lipolysis, proteolysis and sensory properties. *Meat Science, 92*(4), 704–714.

Marinowic, D. R., et al. (2021). A new SYBR Green real-time PCR to detect SARS-CoV-2. *Scientific Reports, 11*(1), 2224–2235.

Meng, F., et al. (2013). Evaluation on the efficacy and immunogenicity of recombinant DNA plasmids expressing spike genes from porcine transmissible gastroenteritis virus and porcine epidemic diarrhea virus. *PLoS One, 8*(3), e57468–e57482.

Meyer, B., et al. (2020). Validation and clinical evaluation of a SARS-CoV-2 surrogate virus neutralisation test (sVNT). *Emerging Microbes & Infections, 9*(1), 2394–2403.

M, M. A., & M, F. D. (2006). Electron beam and gamma irradiation effectively reduce Listeria monocytogenes populations on chopped romaine lettuce. *Journal of Food Protection, 69*(3), 570–574.

Moore, M. A. (2012). Inactivation of enveloped and non-enveloped viruses on seeded human tissues by gamma irradiation. *Cell and Tissue Banking, 13*(3), 401–407.

Mousavi Khaneghah, A., et al. (2020). Electron beam irradiation to reduce the mycotoxin and microbial contaminations of cereal-based products: An overview. *Food and Cosmetics Toxicology, 143*, 111557–111565. https://doi.org/10.1016/j.fct.2020.111557

Palotás, P., et al. (2020). Preservative effect of novel combined treatment with electrolyzed active water and lysozyme enzyme to increase the storage life of vacuum-packaged carp. *Journal of Food Quality*, 1–7, 2020.

Pascual-Iglesias, A., et al. (2019). Recombinant chimeric transmissible gastroenteritis virus (TGEV) - porcine epidemic diarrhea virus (PEDV) virus provides protection against virulent PEDV. *Viruses, 11*(8), 682–700.

Peipei, L., et al. (2020). Cold-chain transportation in the frozen food industry may have caused a recurrence of COVID-19 cases in destination: Successful isolation of SARS-CoV-2 virus from the imported frozen cod package surface. *Biosafety and Health, 2*(4), 199–201.

Perera, R., et al. (2021). Evaluation of a SARS-CoV-2 surrogate virus neutralization test for detection of antibody in human, canine, cat, and Hamster sera. *Journal of Clinical Microbiology, 59*(2), e02504–e02520.

Pillai, S. D., & Shayanfar, S. (2017). Electron beam technology and other irradiation technology applications in the food industry. *Topics in Current Chemistry, 375*(1), 6–26.

Pomeranz, L. E., et al. (2005). Molecular biology of pseudorabies virus: Impact on neurovirology and veterinary medicine. *Microbiology and Molecular Biology Reviews, 69*(3), 462–500.

Praveen, C., et al. (2013). Susceptibility of murine norovirus and hepatitis A virus to electron beam irradiation in oysters and quantifying the reduction in potential infection risks. *Applied and Environmental Microbiology, 79*(12), 3796–3801.

Predmore, A., et al. (2015). Electron beam inactivation of Tulane virus on fresh produce, and mechanism of inactivation of human norovirus surrogates by electron beam irradiation. *International Journal of Food Microbiology, 198*, 28–36.

R, M. K., et al. (2021). Recurrent deletions in the SARS-CoV-2 spike glycoprotein drive antibody escape. *Science, 371*(6534), 1139–1142.

Rodriguez, O., et al. (2006). Surrogates for validation of electron beam irradiation of foods. *Journal International Journal of Food Microbiology, 110*(2), 177-122.

Sanglay, G. C., et al. (2011). Electron-beam inactivation of a norovirus surrogate in fresh produce and model systems. *Journal of Food Protection, 74*(7), 1155–1160.

Schmidt, T., et al. (2012a). Inactivation effect of standard and fractionated electron beam irradiation on enveloped and non-enveloped viruses in a tendon transplant model. *Transfusion Medicine and Hemotherapy, 39*(1), 29–35.

Schmidt, T., et al. (2012b). Inactivation effect of standard and fractionated electron beam irradiation on enveloped and non-enveloped viruses in a tendon transplant model. *Transfusion Medicine and Hemotherapy, 39*(1), 29–35.

Singh, G., et al. (2021a). Monitoring SARS-CoV-2 decontamination by dry heat and ultraviolet treatment with a swine coronavirus as a surrogate. *Infection Prevention in Practise, 3*(1), Article 100103.

Singh, G., et al. (2021b). Monitoring SARS-CoV-2 decontamination by dry heat and ultraviolet treatment with a swine coronavirus as a surrogate. *Infection Prevention in Practice, 3*(1), 100103–100107.

Spyros, L., et al. (2021). The animal origin of SARS-CoV-2. *Science, 373*(6558), 968–970.

Su, Y.-C., et al. (2004). Electron beam irradiation for Reducing Listeria monocytogenes Contamination on cold-smoked salmon. *Journal of Aquatic Food Product Technology, 13*(1), 3–11.

Sun, Y., et al. (2020). Improvement of the quality stability of vacuum-packaged fermented fish (Suanyu) stored at room temperature by irradiation and thermal treatments. *International Journal of Food Science and Technology, 56*(1), 224–232.

Tai, L., et al. (2021). Nanometer-resolution in situ structure of the SARS-CoV-2 postfusion spike protein. *Proceedings of the National Academy of Sciences of the United States of America, 118*(48). https://doi.org/10.12691/ajfst-6-6-2. e2112703118-e2112703126.

Terio, V., et al. (2021a). Survival of a SARS-CoV-2 surrogate on flow-pack polyethylene and polystyrene food trays at refrigeration and room temperature conditions. *Applied Sciences-Basel, 11*(9), 3977–3984.

Terio, V., et al. (2021b). Survival of a SARS-CoV-2 surrogate on flow-pack polyethylene and polystyrene food trays at refrigeration and room temperature conditions. *Applied Sciences, 11*(9), 3977–3984.

Tsai, K. C., et al. (2021). A traditional Chinese medicine formula NRICM101 to target COVID-19 through multiple pathways: A bedside-to-bench study. *Biomedicine & Pharmacotherapy, 133*, 111037–111047.

Vajdi, M., et al. (2019). Using electronic nose to recognize fish spoilage with an optimum classifier. *Journal of Food Measurement and Characterization, 13*(2), 1205–1217.

Yagiz, Y., et al. (2010). Correlation between astaxanthin amount and a* value in fresh Atlantic salmon (Salmo salar) muscle during different irradiation doses. *Food Chemistry, 120*(1), 121–127.

Yao, H., et al. (2020). Molecular architecture of the SARS-CoV-2 virus. *Cell, 183*(3), 730–738.

Yekta, R., et al. (2021). Food products as potential carriers of SARS-CoV-2. *Food Control, 123*, 107754–107765.

Yuan, Q., et al. (2020). A nosocomial COVID-19 outbreak initiated by an infected dockworker at Qingdao city port — shandong Province, China, October, 2020. *China CDC Weekly, 2*(43), 838–840.

Yuhua, C., et al. (2021). Transmission of SARS-CoV-2 on cold-chain food overpacks: A new challenge. *Journal of global health, 11*. https://doi.org/10.7189/jogh.11.03071, 03071-03075.

Zhang, Q. Q., et al. (2017). Combined effect of polyphenol-Chitosan Coating and irradiation on the microbial and sensory quality of carp fillets. *Journal of Food Science, 82*(9), 2121–2127.

Zhu, Y., et al. (2017). A sensitive duplex nanoparticle-assisted PCR assay for identifying porcine epidemic diarrhea virus and porcine transmissible gastroenteritis virus from clinical specimens. *Virus Genes, 53*(1), 71–76.